3-2 Polarimetric Rainfall Observation with CAMPR (CRL Airborne Multiparameter Precipitation Radar)

HANADO Hiroshi, SATOH Shinsuke, NAKAGAWA Katsuhiro

Rainfall observation was conducted with an airborne rain radar named CAMPR (CRL Airborne Multiparameter Precipitation Radar) during WMO-01 (Winter MCSs Observations over the Japan Sea-2001). Hydrometeor discrimination in rain system over the Japan Sea at winter season was examined with vertical profiles of polarimetric radar observables obtained with CAMPR.

Keywords
Multiparameter radar, Airborne rain radar, Discrimination of hydrometeors, $\rho_{HV}(0)$ (cross correlation coefficient), LDR (linear depolarization ratio)

1 Rainfall and snowfall observation using polarimetric radar

Radars with polarization diversity have a variable transmitted and/or received wave polarization, or provide for dual channel reception of orthogonally polarized waves. This allows measurement of hydrometeor characteristics such as size, shape, spatial orientation, and discrimination of thermodynamic phase. Various hydrometeor types, such as raindrops, ice crystals, snowflakes, hail, or graupel, may be identified based on differences in scattered echo by the particles. In recent years, a number of researchers have focused on polarimetric information on hydrometeors[1] as a potential source for an improved understanding of physical processes within precipitating cloud systems and improved rainfall rate estimation. Regarding raindrops, small drops (of 1 mm or less in diameter) are spherical, dominated by the surface tension of water, while large ones (2-7 mm in diameter) become oblate due to frictional forces arising from their motion relative to the air[2]. Researchers have attempted to estimate the distribution of drop sizes and to increase the accuracy of estimates regarding rainfall rates, based on a property that the backscattering of oblate raindrop at horizontal polarization is stronger than that at vertical polarization. In propagation (forward scattering), the degree of phase rotation of electromagnetic waves differs between at horizontal and at vertical polarization. This feature has been used for a method of estimating rainfall rate insensitive to differences in drop size distribution, and for a method of attenuation correction in case of heavy rainfall[1][3]. Ice particles present a more complex case. The basic shape of the ice crystal depends on the temperature and relative humidity of the air in which it develops. In the (0℃, −3℃) and (−8℃,−25℃) approximate intervals, plates or dendrites crystals form if the humidity is high. In the (−3℃,−8℃) and (< −25℃) intervals, columns or needles from if the humidity is high[4]. If the shape of ice particles is known from the polarimetric characteristics in radar echo, the creation/growth process and ambient weather conditions can in turn be estimated. This makes it possible to clarify the physics of precipitating clouds. As in the case of ice crystals, knowing the shapes

of hydrometeor forms such as snow, hail, and graupel particles improves our understanding of meteorological phenomena. In particular, with respect to hail, there is demand for reliable methods of detection and prediction in order to avert damage to agricultural crops. Polarimetric radar has been investigated as a promising tool to this end. In this paper, we have tried to identify each hydrometeos type in precipitating clouds over the Japan Sea in winter, based on polarimetric measurement data taken in flight tests using CRL Airborne Multiparameter Precipitation Radar (CAMPR).

2 CRL Airborne Multiparameter Precipitation Radar (CAMPR)

The CAMPR system[5], which uses the Ku-band frequency (13.8 GHz) also employed by TRMM (Tropical Rainfall Measuring Mission) Precipitation Radar[6], was developed to validate the capabilities of TRMM precipitation radar[7]. A dual beam antenna for airborne experiments CAMPR-D, installed in 1997, makes it possible to perform either dual Doppler or polarimetric observations of rainfall[8][9]. Table 1 lists the major specifications of the CAMPR system. In the CAMPR-D, two beams (forward and nadir beams) are available, with the nadir beam is available at both horizontal (H) and vertical (V) polarization. Two transmit polarization sequences, HV and HHVV, are selective, and two horizontal and vertical receivers simultaneously capture copolar and cross-polar components of radar echo. The data acquisition system has two modes: (a) an integral mode that can use both intensity and Doppler information on radar echo, Doppler velocity and spectrum width estimated with pulse pair method, and (b) an all-hit mode that can record successive in-phase and quadrature phase components of radar echo (max. 1024 hits). In case of integral mode, the correlation coefficient between horizontal and vertical polarization is not recorded, but the intensity and Doppler information are recorded almost continuously because the amount of recorded data is relatively small owing to data averaging in hardware. In case of all-hit mode, the amount of captured data is so large that the data transfer time needs and its recorded data is intermittent. However, in the December 2000, a replacement of the computer in the data acquisition system has helped reduce the above disadvantage by increasing data transfer and recording rate. This paper uses the data captured by all-hit mode.

Table 1 *Major CAMPR specifications*

Frequency	13.8 GHz (Ku-Band)
Transmitter	TWTA 2kW (peak)
Receiver	2 sets (one is for H, the other is for V or Forward Beam)
Pulse Width	0.5, 1, 2 μsec
Range Resolution	75, 150, 300 m
PRF	2, 4, 8 kHz
Doppler Unaliased Speed	10.9, 21.7, 43.4 m/sec
Transmit Polarization Sequence	H, V, HV, HHVV or F, HF, HHFF
Data Acquisition Mode	(a) Integral Mode (b) All Hit Mode (max 1024 hits)
Antenna Mode	(a) Dual Beam (HF) mode (b) Polarization (HV) Mode

3 Rainfall observation with CAMPR-D multiparameter radar

CAMPR-D is capable of beam scanning over a wide range by mechanically rotating the antenna in its radome. The beam scan range is 60 degrees on the right side of the aircraft and 85 degrees on the left, as measured from the nadir direction, as shown in Fig.1(a). For hydrometeor observations using polarimetric radar, typically measured are the radar reflection factor (Z) for co-polarization (horizontal polarization in most weather radar systems); the differential reflectivity between horizontal and vertical polarization, ZDR ($=Z_{HH}/Z_{VV}$), which results from the flattening of rain drops caused by their motion relative to the air; the differential propagation phase between horizontal and vertical polarization, ΦDP (and its derivative in the range direction, KDP), the intensity ratio, LDR (=linear depolarization ratio=Z_{HV}/Z_{HH}), between cross-polar

and copolar radar reflectivity, which also results from the non-spherical shape of drops; and the cross correlation coefficient, ρ_{HV} (0), between horizontal and vertical polarization radar echo[1][3]. Among these parameters, ZDR, ϕDP, and KDP are related to differences between the horizontal and vertical dimensions of hydrometeor particles. These parameters can be measured when the radar beam is directed close to horizontal. However, when the beam is directed close to vertical, these parameters cannot be measured if the hydrometeors are oriented randomly. Given these characteristics of CAMPR-D, we have summarized in Table 2 the effects of beam direction for polarimetric observation using CAMPR-D. In terms of polarimetric observation, the nadir beam has the disadvantage, compared to the horizontal beam, of providing data of fewer variables.

Nevertheless, due to the data characteristics of CAMPR-D (see Fig.1(b)), it offers the advantage of the radar's range resolution becoming the vertical resolution of the data actually measured. This vertical resolution can be as high as 150 m, made possible by a pulse width (1 μsec.) that is usually available in flight experiments using CAMPR-D. In contrast, the horizontal beam has the advantage of providing data of many polarimetric variables. However, the antenna beam width (about 7 degrees) of CAMPR-D results in a horizontal beam widening of 700m or so at a range of 6 km, which adversely affects vertical resolution. Moreover, when measurements are performed at high altitudes in the sky along the horizontal beam, it must travel a considerable distance to the melting layer, the target of polarimetric measurements. It means that the data quality of returned signals is relatively low. Taking into account all these advantages and disadvantages, we decided to use data provided by the nadir beam for the current analysis.

4 Hydrometeor-type classification with polarimetric radar observables

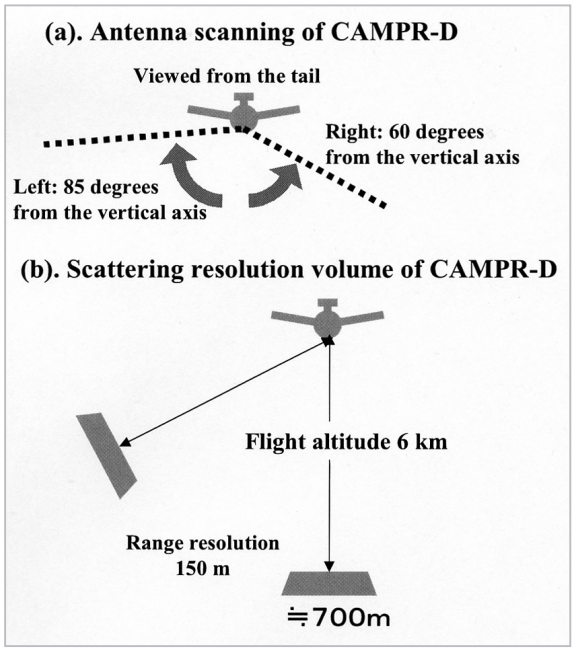

Fig.1 *Antenna scanning and measurable volume of CAMPR-D*

Table 2 *Aircraft-based polarimetric measurement using CAMPR-D*

Beam	Observables	Advantage	Disadvantage
Nadir	Z, ρ_{HV} (0), LDR	High vertical resolution	Fewer observables
Horizontal	Z, ρ_{HV} (0), LDR ZDR ϕDP KDP	Many observables	Low vertical resolution Poor sensitivity near the ground

For hydrometeor-type classification, the relationship between polarimetric radar observables and kind of hydrometeors are summarized in Table 3. The information provided in this table with respect to Z, ρ_{HV} (0), and LDR used in our research has been excerpted from Doviak and Zrnic (1993)[3]. Table 3 indicates that the linear depolarization ratio (LDR) of raindrops is small, and that the correlation coefficient between horizontally and vertically polarized returned signals, ρ_{HV} (0), approaches 1 due to their geometric symmetry. In wet-melting snow often observed in the melting layer, the cross-polar component of returned signals grows large. LDR grows and the correlation coefficient ρ_{HV} (0) decreases from 1 to around 0.8. In hail, the cross-

polar component is large and LDR grows, while the correlation coefficient remains around 0.95, with no significant decline. Unlike the results of CAMPR measurement using the Ku band, the figures in Table 3 are for another measurement using an S-band (i.e., lower frequency than Ku band) polarimetric radar; thus the figures differ slightly. Nevertheless, they provide sufficiently useful information for understandings of changes in LDR and ρ_{HV} (0) across the melting layer. In CAMPR-D, the LDR limit is estimated to be around -25dB from the polarimetric antenna . Thus, unless S/N for the rainfall echo is enough high, observed LDR values is meaningless. Meanwhile, ρ_{HV} (0) may be estimated with satisfactory accuracy even when S/N in the rainfall echo is not high, since it derives from copolar components.

5 Polarimetric rainfall observation over the Japan Sea during winter in WMO-01[10](Winter MCSs Observations over the Japan Sea-2001)

In a flight experiment for snowfall observation, which was a part of WMO-01 (Winter MCSs Observations over the Japan Sea-2001), we used a KingAir equipped with CAMPR-D and a Gulfstream Jet equipped with SPIDER (Special Polarimetric Ice Detection and Explication Radar) and a particle probe, as well as meteorological measurement instruments (provided by the Meteorological Research Institute) on the afternoon of January 27, 2001. These aircraft flew the same course along 137.30 ˚E longitude during the same period of time. Fig.2 shows the flight course.

The KingAir equipped with CAMPR flew south to north (latitude 36.7 ˚N to 39 ˚N) from 13:45 to 14:15 at an altitude of 6 km. The Gulfstream Jet equipped with the particle probe and SPIDER took flight somewhat earlier, 12:34-12:49, from south to north (latitude 37.4 ˚N to 39.2 ˚N) at an altitude of 10.2 km. The Gulfstream Jet continued to fly along longitude 137.30 ˚E at altitudes of 3.6, 1.5, and 0.3 km to measure the internal structure of cloud systems by using the particle probe[10]. The KingAir equipped with CAMPR was a propeller plane, while the Gulfstream Jet

Table 3 *Values of Polarimetric Measurands for Various Precipitation Types*

Types	Z (dBZ)	ρ_{HV} (0)	LDR
Drizzle	< 25	> 0.99	< -34
Rain	25 to 60	> 0.97	-34 to -27
Snow, dry, low density	< 35	> 0.99	< -34
Crystals, dry, high density	< 25	> 0.95	-34 to -25
Snow, wet melting	< 45	0.8 to 0.95	-18 to -13
Graupel, dry	40 to 50	> 0.99	< -30
Graupel, wet	40 to 55	> 0.99	-25 to -20
Hail, small < 2cm, wet	50 to 60	> 0.95	< -20
Hail, large > 2cm, wet	55 to 70	> 0.96	-15 to -10
Rain & Hail	50 to 70	> 0.9	-20 to -10

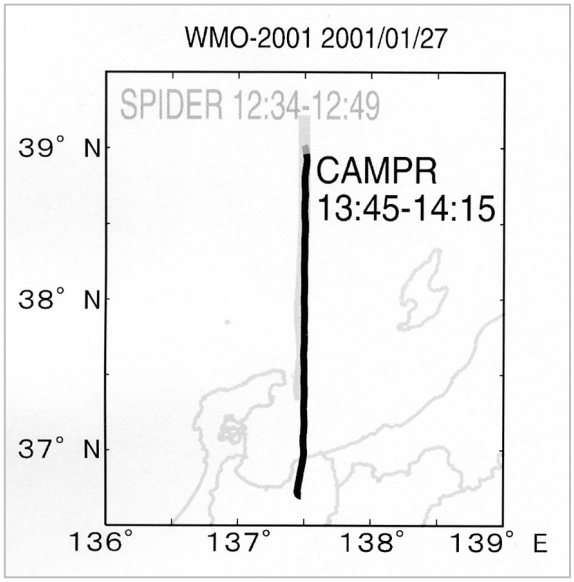

Fig.2 *Flight course of the KingAir equipped with CAMPR and the Gulfstream Jet equipped with SPIDER, a particle probe, and meteorological measurement instruments*

equipped with SPIDER was a jet one. Thus, their cruising speeds were significantly different: the Gulfstream Jet took 15 minutes to fly along the flight path shown in Fig.2,while the KingAir took 30 minutes. CAMPR used polarimetric observation mode, fixing the antenna beam in the nadir direction and collecting data by using the all-hit mode in data acquisition. The transmit pulse width was 1 μsec, and the range resolution (vertical resolution) was 150 meters. Since horizontal and vertical polarization wave pulses were transmitted alternately, the transmit PRF (pulse repetition frequency) was 4 kHz, while that of horizontal polarization alone was equivalent to 2 kHz, and the Doppler aliasing frequency was about ±10 m/sec. Each record consisted of 1024 hits, and the record intervals were 2.4 sec, or about 190 m horizontally. As demonstrated in Fig.1(b), the CAMPR-D scattering resolution volume for nadir measurements at an altitude of 6 km was 700 m horizontally. Thus, we believe there are no significant gaps in this measurement. Fig.3 shows the vertical cross-sections of rainfall echo observed by CAMPR. The lateral axis represents the horizontal distance along the longitude 137.30 ˚E, with the left side of the figure representing south (altitude 36.8 ˚N) and the right representing north (altitude 39 ˚N). The total flight path was about 240 km, since the aircraft flew about 30 minutes at a speed of about 130 m/sec. The vertical axis represents the altitude. The sea surface corresponded to 0 km; the top is the altitude of 6 km, where the aircraft flew; and the bottom is 2 km below the sea surface. The undersea echo is called “mirror echo.” Here, a radio wave is emitted from the radar, reflected from the sea surface, scattered by rain in the sky, then reflected once again from the surface, thus returning to the radar after being reflected twice on the surface, and mirroring the real echo across the surface. In Fig.3, the top plate shows radar reflection factor Z_{VV} of the copolar component (vertical transmission/reception); the middle plate is radar reflection factor Z_{HV} of cross-polar component (horizontal transmission, vertical reception); the bottom plate is the correlation between horizontal and vertical polarization, ρHV (0). A sea surface echo is seen in these figures at around zero km in altitude. A rain echo is also recognized above the sea surface up to 4 to 5 km (see the copolar component Z_{VV} at the top plate of Fig.3). The strong echo near the aircraft (at an altitude of about 6 km) is caused by the leakage of the transmit power. A blurred mirror-image echo is also seen under the seasurface echo in the region where the rainfall echo was strong.

Listed below are points in the characteristics of observed rainfall echoes shown in Fig.3.

Copolar component (Zvv):

(a) There exists an echo peak that probably indicates the existence of a melting layer. Its altitude changes from 300 to 800 m above sea surface.

(b) The above melting layer altitude is highest near the center (latitude 38 ˚N) region in the figure and likely to be lower on its south and north sides.

(c) There exists a stripe pattern rising toward north in the sky over the land region (as shown in the left half of the figure).

Cross-polar component (Zhv):

(d) There is an echo at almost the same altitude of the melting layer altitude detected by the copolar component.

(e) The thickness of the observed melting layer is larger over and near the land region

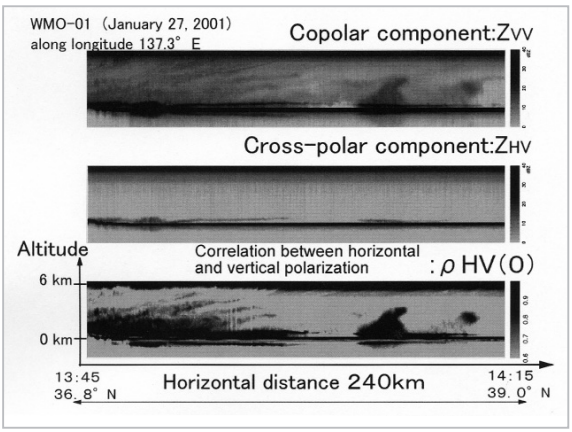

Fig.3 *Polarimetric measurement of rainfall using CAMPR in WMO-01 experiment conducted over the Japan Sea (January 27, 2001)*

(as shown left in the figure) than that of offshore region.

Correlation coefficient (ρ_{HV} (0)):

(f) Has a pattern similar to the copolar component.

(g) There appears to be a peak corresponding to the melting layer detected by the copolar component.

The altitude changes (a), (b) of the melting layer indicated by the copolar component were also recognized in in-situ atmospheric measurements using meteorological instruments installed in the Gulfstream Jet. According to an analysis of a mesocyclone in the Japan Sea on the day based on both the cloud radar (SPIDER) observation and the meteorological observation with the Gulfstream Jet[10], the mesocyclone developed in the Japan Sea between Noto Peninsula and Sado Island when a south low-pressure system passed by the south coast of Japan, and the mesocyclone moved slowly to the northeast. The core of the small low-pressure system was warmer than the surrounding area, approximately 2 to 3 K higher in equivalent potential temperature. The rainfall region obtained by SPIDER was concentrated in both north and south sides of the mesocyclone where the gradient of equivalent potential temperature was large. The rain echo in the top plate of Fig.3 observed by CAMPR was weak around latitude 38 ˚N where the melting layer was highest, while the rain echo was strong on its south and north sides. Thus, two different radars, CAMPR and SPIDER, observed the same mesocyclone. The altitude difference of 500 m detected by CAMPR radar echo agreed with the difference in equivalent potential temperature (2 to 3 K) measured by meteorological instruments aboard the Gulfstream Jet.

The regular (stripe) structure of the rain echo (c) was not investigated in detail in this study. However, since its area of occurrence is limited to areas near land, its origin might be land or mountainous terrain. In the property (d), the cross-polar component was large near the melting layer. This agrees with conventional observations obtained from LDR measurements. The difference in thickness of the melting layer (e) may suggest a difference in atmospheric turbulence at the altitude of the melting layer, and should be investigated in the future. In terms of (f), the correlation was equal to almost 1 in areas where the rain echo was recognized, but close to zero where no echo was recognized. This result agrees with conventional observations. The characteristic noted in (g) — the coincidence of peaks between the copolar component and correlation component — appears to contradict the ordinary observation results showing that Z and LDR indicate peaks in the melting layer, while ρ_{HV} (0) shows a negative peak. Thus, we examined the vertical profile of the three variables in the following section in detail.

6 Vertical profile of polarimetric observables and hydrometeors classification

Fig.4 shows the vertical profiles of the radar reflectivity factor (Z), linear depolarization ratio (LDR) and copolar correlation coef-

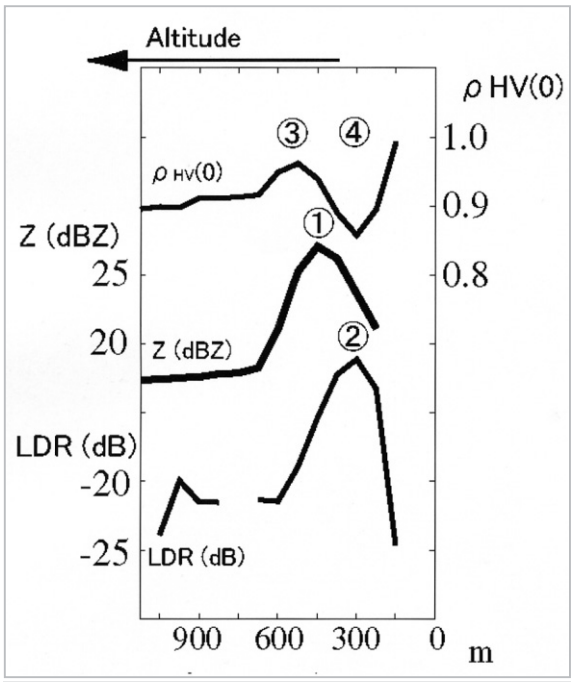

Fig.4 *Vertical profiles of radar reflective factor (Z), linear depolarization ratio (LDR) and copolar correlation coefficient (ρ_{HV}(0)) (Lateral axis represents the altitude above sealevel.)*

ficient (ρ_{HV} (0)) for rainfall area near latitude 38.30 ˚N, which are shown on the right side of Fig.3.

In Fig.4, the lateral axis represents the altitude above sealevel, where the right end represents the sea surface and left end represents an altitude of 1200 m. The CAMPR data has a range resolution of 150 m determined by the pulse width. However, since the data was subject to oversampling at twice the frequency in the range direction, data was sampled at every 75 m, as shown in Fig.4. In Fig.3, the copolar component, cross-polar component, and correlation coefficient appeared to have peaks at almost the same altitude. However, if the data is expanded vertically, the positive peak ① of the radar reflectivity factor: Z, the positive peak ② of the LDR, the positive peak ③ of the correlation coefficient $\rho_{HV}(0)$, and the negative peak ④ of the $\rho_{HV}(0)$ lying below ③ have differing altitudes. The Z positive peak ①, which is also recognized as "blind-band"using conventional weather radar, lies at an altitude of 450 m. Both the LDR positive peak ② and the $\rho_{HV}(0)$ negative peak ④ lie at an altitude of 300 m, which corresponds to a melting layer. These results agree with conventional observation results in which Z and LDR show positive peaks near a melting layer, while ρ_{HV} (0) has a negative peak, and the Z peak lies at an altitude slightly higher than that of the LDR and ρ_{HV} (0) peaks. The $\rho_{HV}(0)$ positive peak ③ that appeared to correspond to the Z positive peak ① in Fig.3 lies at an altitude of 525 m, which is slightly higher than that of the Z positive peak ①. It is difficult to provide a clear explanation for the ρ_{HV} (0) positive peak ③; however, since it shows a high correlation, it may indicate that the hydrometeors are actually somewhat spherical. There is no specific decrease (negative peak) of LDR in the position of peak ③. This result does not agree with the conclusion[1] that LDR and ρ_{HV} (0) have a one-to-one relationship if there is azimuthal symmetry in the distribution of hydrometeors. Thus, the current observation result may suggest that there is no azimuthal symmetry in the distribution of hydrometeors and that hydrometeors are oriented in a specific direction — non-spherical hydrometeors are arrayed in a specific direction.

Finally, we attempted to identify hydrometeor types based on the relationship between values of polarimetric measurands and various precipitation types listed in Table 3. Table 3 lists the results provided by measurement using S-band weather radar and may be slightly different from the results measured with the Ku-band. However, the basic characteristics should not differ much. Table 4 summarizes the results of hydrometeors classification. Table 4 provides the following insights that agree with conventional ones. Dry hydrometeors existing at high densities at high altitudes gradually melt on the surface as they fall and temperature rises. Wet particles easily stick to each other and grow in size through collision. This increases the power of the returned signal, while the particle density decreases. When the wet particles further melt and finally become raindrops, the apparent volume decreases and the radar reflectivity factor decreases, while the falling speed grows. As a result, the radar reflectivity factor is made even smaller, since the particle density per unit volume decreases.

Table 4 *Discrimination of hydrometeors based on polarimetric observables*

Altitude	Features	Hydrometeor Type
600 m or higher	$\rho_{HV}(0)$ 0.9; both Z and LDR are small	Crystals, dry, high density
500 m	Peak of $\rho_{HV}(0)$	Snow, dry, low density
450 m	Peak of Z factor	Snow, wet melting
300 m	$\rho_{HV}(0)$ has a negative peak; LDR has a peak	
Less than 300 m	$\rho_{HV}(0)$ 1.0; small LDR	Rain

7 Summary and future challenges

We attempted to identify hydrometeor types based on polarimetric data provided by CRL Airborne Multiparameter Precipitation Radar (CAMPR-D) measurements conducted over the Japan Sea in winter. Most of the obtained insights agreed with conventional observations provided by polarimetric measurements. However, one result — the detection of a positive peak of ρ_{HV} (0) in the upper melting layer, with no corresponding negative LDR peak — may include additional information with respect to hydrometeors existing in the upper melting layer. We plan to compare this data with other observations and calculations for the detailed scattering properties of hydrometeors.

Acknowledgments

We are grateful to Nakanihon Air Service Co., Ltd. for their cooperation in flight services for the field experiments. We thank the staff members of CREST for their assistance with flight tests.

Japan Science and Technology Corporation — Core Research for Evolutional Science and Technology, "Studies on Structure and Formation/Development Mechanisms of Mesoscale Convective Systems", supported this experiment.

References

1 V. N. Bringi and V. Chandrasekar, "Polarimetric Doppler Weather Radar", Cambridge University Press, 2001.

2 Hans R. Pruppacher and James D. Klett, "Microphysics of Clouds and Precipitation", Second Revised and Enlarged Edition with an Introduction to Cloud Chemistry and Cloud Electricity, Kluwer Academic Publishers, 1997.

3 Richard J. Doviak and Dusan S. Zrnic, "Doppler Radar and Weather Observations", Second Edition, Academic Press Inc., 1993.

4 Henri Sauvageot, Radar Meteorology, Artech House Inc., 1992.

5 H. Kumagai, K. Nakamura, H. Hanado, K. Okamoto, N. Hosaka, N. Miyano, T. Kozu, N. Takahashi, T. Iguchi, and H. Miyauchi, "CRL airborne multiparameter precipitation radar (CAMPR): System description and preliminary results", IEICE Trans. Com., 1996, 770-778, Vol.E79-B.

6 Kozu, T., T. Kawanishi, H. Kuroiwa, M. Kojima, K. Oikawa, H. Kumagai, K. Okamoto, M. Okumura, H. Nakatsuka, and K. Nishikawa, "Development of precipitation radar onboard the Tropical Rainfall Measuring Mission (TRMM) satellite", IEEE Trans. Geosci. Remote Sensing, 39, 102-116, 2001.

7 Kenji Nakamura ,Hiroshi Hanado, and Kinji Furukawa, "Report of the Ishigaki/Miyako Campaign Experiment for TRMM (IMCET) 1998", NASDA EORC Bulletin Technical Report, 1999, 1-76, No.3.

8 Satoh, S, H. Hanado, K. Nakagawa, T. Iguchi, K. Nakamura, and M. Yoshizaki, "Airborne Multiparameter Precipitation Radar (CAMPR) Observation of Wind Fields in Snow Clouds", This Special Issue of CRL Journal.

9 Timothy K. Isiah, T. Iguchi, Y. Ohsaki, H. Horie, H. Hanado, and H. Kumagai, "Test of the Specific Differential Propagation Phase Shift (KDP) Technique for Rain-Rate Estimation with a Ku-Band Rain Radar", J. Atmos. Ocean. Tech, 1999, 1077-1091, Vol.16.

10 Yoshizaki, M., T. Kato, H. Eito, A. Adachi, M. Murakami, S. Hayashi and WMO-01 Observation Group, 2001a: A report on "Winter MCSs (mesoscale convective systems) observations over the Japan Sea in January 2001 (WMO-01)" (in Japanese). Tenki, 48, 893-903, 2001.

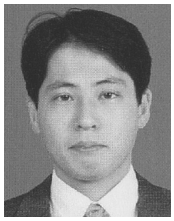

HANADO Hiroshi

Senior Researcher, Precipitation Radar Group, Applied Research and Standards Division

Microwave Remote Sensing

***NAKAGAWA Katsuhiro**, Dr. Eng.*

Senior Researcher, Subtropical Environment Group, Applied Research and Standards Division

Radar Hydrology

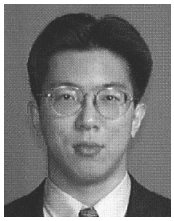

***SATOH Shinsuke**, Dr. Sci.*

Senior Researcher, Precipitation Radar Group, Applied Research and Standards Division

Radar Meteorology